

Reversed Doppler Effect in Photonic Crystals

Evan J. Reed,* Marin Soljačić, and John D. Joannopoulos

Department of Physics, Massachusetts Institute of Technology, Cambridge, Massachusetts 02139, USA

(Received 6 March 2003; published 23 September 2003)

Nonrelativistic reversed Doppler shifts have never been observed in nature and have only been speculated to occur in pathological systems with simultaneously negative effective permittivity and permeability. This Letter presents a different, new physical phenomenon that leads to a nonrelativistic reversed Doppler shift in light. It arises when light is reflected from a moving shock wave propagating through a photonic crystal. In addition to reflection of a single frequency, multiple discrete reflected frequencies or a 10 GHz periodic modulation can also be observed when a single carrier frequency of wavelength $1 \mu\text{m}$ is incident.

DOI: 10.1103/PhysRevLett.91.133901

PACS numbers: 42.70.Qs, 42.79.Hp, 42.79.Jq, 47.40.Nm

In 1843, Johann Christian Doppler proposed an effect whereby the frequency of waves emitted from a moving object is shifted from the source frequency. The Doppler shift phenomenon has since realized applications ranging from weather and aircraft radar systems to satellite global positioning systems to the measurement of blood flow in unborn fetal vessels to the detection of extrasolar planets. The Doppler effect predicts that light shined by an observer onto an object moving toward him will be reflected with a higher frequency. In this Letter, we show that the established theory behind the Doppler shift breaks down for light reflected from a shock wave propagating in a photonic crystal [1,2], or material with a periodic modulation of the dielectric. We employ detailed numerical simulations and analytical theory to prove that anomalous Doppler shifts, both in sign and magnitude, can be observed. These effects are realizable under readily experimentally accessible conditions. Anomalous Doppler effects have been observed in plasmas that propagate at near-relativistic speeds [3] and have been predicted to occur in pathological systems with simultaneously negative effective permittivity and permeability [4,5]. The anomalous Doppler effects presented in this Letter have a fundamentally different physical origin and can be observed at nonrelativistic speeds in systems with linear optical materials. In the shocked photonic crystal system, 100% of the incident light energy can be transferred into the anomalous Doppler shift.

To explore the phenomena associated with light scattering from a shock wave in a photonic crystal, we perform finite-difference time-domain (FDTD) [6] simulations of Maxwell's equations in one dimension, single polarization, and normal incidence for a system described by a time-dependent dielectric $\epsilon(x, t)$. These simulations solve Maxwell's equations with no approximations except for the discretization, and are known to excellently reproduce experiments.

The effects of a shock wave propagating in a 1D photonic crystal are shown in Fig. 1. The preshocked crystal (on the right) is comprised of two materials with

identical elastic moduli and sound speeds, but differing dielectric. One layer has length $d_1 = 0.2a$ and the other has length $d_2 = 0.8a$, where a is the preshock lattice constant. The compression of the lattice by the shock wave has two key effects on the photonic crystal: The lattice is compressed and the dielectric is changed through a strain dependence. If we focus on materials where the dielectric constant is increased with compression, these two main effects affect the band gap frequency in opposing ways in the shock-compressed material: Decrease of the lattice constant increases the band gap frequency, but increasing the dielectric lowers the band gap frequency. The band gap can be made to decrease in frequency upon compression if materials with a sufficiently large dielectric dependence on strain are employed, $\frac{d\epsilon}{ds}$, where material strain is given by s .

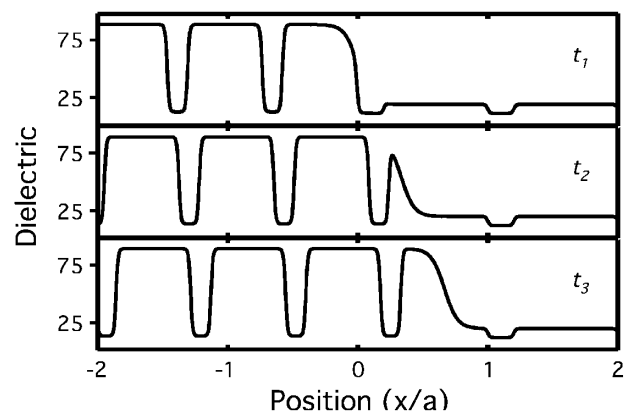


FIG. 1. Dielectric as a function of position for three equally spaced instants in time, $t_1 < t_2 < t_3$. The shock front moves at a constant velocity, and the material behind the shock moves at a smaller constant velocity. For this model, the dielectric ranges from 2.1 to 11.0 before the shock front and 3.7 to 89.4 behind the shock front. These large values are for computational tractability only. All the results of this work can be observed with physically accessible values as discussed in the text.

Materials that are used for acousto-optical modulation, in particular, can have a large negative dielectric dependence on strain [7]. As an illustrative example, we have chosen parameters for our model system with $(1/\epsilon_1)[(d\epsilon_1)/(ds_1)] = -2.9$ and $(1/\epsilon_2)[(d\epsilon_2)/(ds_2)] = -26.5$, an elastic modulus for both materials of 37 GPa, and a shock pressure of 10 GPa. The strain dependence of the dielectric is exaggerated purely due to the computational requirement of very long simulations and fine spatial discretization for realistic parameters. All effects proposed in this paper can be observed in experimentally accessible scenarios. For example, a photonic crystal with a band gap width of $10^{-2}\omega_{\text{gap}}$ made mostly of tellurium shocked to a strain of around 1% will produce frequency shifts of $3 \times 10^{-7}\omega$ which are readily observable experimentally. Experimental details will be discussed later.

The time-dependent 1D dielectric shown in Fig. 1 is composed of bilayer regions where the location of the interfaces between bilayers in the shocked crystal $(x_{1,j}(\hat{t}), x_{2,j}(\hat{t}))$ (in units of the preshocked lattice constant a) is given in terms of the locations of the interfaces between bilayer regions in the unshocked crystal $(\tilde{x}_{1,j}, \tilde{x}_{2,j})$ as

$$x_{i,j}(\hat{t}) = \tilde{x}_{i,j} - \frac{p}{2B}(\tilde{x}_{i,j} - v\hat{t})\{\tanh[-\gamma(\tilde{x}_{i,j} - v\hat{t})] + 1\}. \quad (1)$$

The shock speed is v , the shock front thickness is given by γ^{-1} , the final shock pressure by p , and the elastic modulus for both materials by B . The time has units of $\hat{t} \equiv at/c$. The variation of $\epsilon(\hat{x} \equiv \frac{x}{a})$ in the shocked crystal is given in terms of the bilayer interfaces as [neglecting the strain dependence of $\epsilon(\hat{x})$]

$$\begin{aligned} \epsilon(\hat{x}, \hat{t}) &= \frac{1}{2}(\epsilon_1 + \epsilon_2) + \frac{1}{2}(\epsilon_2 - \epsilon_1) \tanh[\delta(\hat{x} - x_{1,j})], & \frac{1}{2}(x_{1,j} + x_{2,j-1}) \leq \hat{x} < \frac{1}{2}(x_{2,j} + x_{1,j}), \\ \epsilon(\hat{x}, \hat{t}) &= \frac{1}{2}(\epsilon_1 + \epsilon_2) + \frac{1}{2}(\epsilon_2 - \epsilon_1) \tanh[-\delta(\hat{x} - x_{2,j})], & \frac{1}{2}(x_{2,j} + x_{1,j}) \leq \hat{x} < \frac{1}{2}(x_{1,j+1} + x_{2,j}). \end{aligned} \quad (2)$$

The time dependence of ϵ enters from the time dependence of the dielectric region interfaces, $[x_{1,j}(\hat{t}), x_{2,j}(\hat{t})]$. The dielectric alternates between ϵ_1 and ϵ_2 with tanh splines of width δ^{-1} between regions to prevent a moving discontinuity. To account for the strain dependence of the two dielectric regions, we apply a transform to the dielectric given by Eq. (2),

$$\epsilon(\hat{x}, \hat{t}) \rightarrow \epsilon(\hat{x}, \hat{t}) \left[1 + \left(\frac{1}{\epsilon_1} \frac{d\epsilon_1}{ds_1} + \left(\frac{1}{\epsilon_2} \frac{d\epsilon_2}{ds_2} - \frac{1}{\epsilon_1} \frac{d\epsilon_1}{ds_1} \right) \frac{(\epsilon(\hat{x}, \hat{t}) - \epsilon_1)}{(\epsilon_2 - \epsilon_1)} \right) \frac{p}{2B} (\tanh(-\gamma(\hat{x} - v\hat{t})) + 1) \right]. \quad (3)$$

In Fig. 1, the thickness of the shock wave front (γ^{-1}) is 1, $\delta^{-1} = \frac{1}{60}$. Figure 2 is a schematic of the band gap frequencies in front of and behind the shock front for the dielectric given in Fig. 1. The first band gap is lowered in frequency as the shock compresses the photonic crystal. Consider now continuous-wave electromagnetic radiation incident from the right (opposite to the direction of shock propagation) with frequency within the first band gap of the postshock crystal as shown in Fig. 2. The frequency of this radiation is far from the first band gap edge in the preshock crystal. The incident light is reflected and acquires a *reversed* Doppler shift, i.e., lowered frequency in this case.

Figure 3 shows the absolute value of the magnetic field for a FDTD simulation where this reversed Doppler effect is observed. The shock front (dashed line) has thickness $\gamma^{-1} = 2$ and propagates to the right with $v = 1.5 \times 10^{-2}c$, which is chosen to be artificially high for computational considerations. The panels in Fig. 3 are obtained by Fourier transforming the magnetic field over windows of time ($\Delta t = 500a/c$) beginning at the times shown in the upper right corners. The top panel shows light incident from a source on the right, and the bottom panel shows this light reflecting with a decreased frequency.

Figure 4 shows a similar FDTD simulation where the shock front is considerably sharper, $\gamma^{-1} = 0.1$.

Here, $v = 3 \times 10^{-3}c$ and the Fourier transform is performed over a time ($\Delta t = 3500a/c$). Multiple, equally spaced reflected frequencies are observed in this case. These frequencies are a result of the time-periodic nature of the shock propagation over a periodic structure. The interpretation of the reflected light as multiple equally spaced frequencies or a temporally periodic modulation of a single carrier frequency is a matter of resolution in the experimental apparatus. For light of $1 \mu\text{m}$

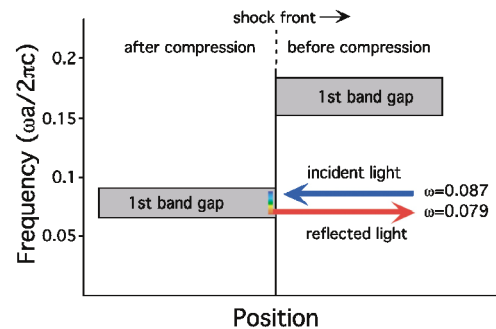


FIG. 2 (color). Schematic of a shock wave moving to the right that compresses the lattice but lowers the band gap frequency due to a strain dependence of the dielectric. Light incident from the right reflects from the post-shock band gap with a *reversed* Doppler shift.

wavelength, the periodic modulation has a frequency around 10 GHz.

The new physics presented here can be understood in terms of a simple analytical theory. We focus on a scenario where the incident light is at a frequency that falls within the gap of the postshock, *compressed* crystal. We choose the incident light frequency to be far below the band gap of the preshock crystal, where it may be described by plane waves. An effective model of the shock front is a mirror with a space-dependent E field reflection coefficient, $R(x)$, where x is the mirror position. R has the property that $|R(x)| = 1$ since the incident light reflects from the band gap of the postshock crystal. In general R has some frequency dependence, but we will consider the bandwidth of the incident light sufficiently small to neglect it. If the shock front is stationary, the condition on the electric field at the shock front in terms of incident and reflected light is

$$\sum_j E_j e^{-i(\omega_j t - k_j x)} = R(x) E_0 e^{-i(\omega_0 t + k_0 x)}, \quad (4)$$

where k_0 and k_j correspond to the respective incident and reflected wave vectors in the preshock medium and E_0 and E_j are constants. The reflection coefficient $R(x)$ can be written $R(x) = \sum_G \beta_G e^{-iGx}$, which is the most general form with the property that $R(x)$ is periodic in the preshock lattice, $R(x) = R(x + a)$. The reciprocal lattice vectors G are $2\pi q/a$, where q is an integer. This substitution and letting $x \rightarrow x_0 + vt$, where v is the shock speed, yield the frequency shifts required by the time dependence of Eq. (4) in the nonrelativistic limit,

$$\omega_G - \omega_0 = (2k_0 + G)v. \quad (5)$$

The reflected light has frequency components ω_G that differ from the usual Doppler shift, $2k_0 v$, by the amount Gv . The amplitude of each of the reflected components is

$$|E_G| = |\beta_G| |E_0|. \quad (6)$$

When $R(x)$ pertains to the ℓ th band gap, one can readily show that $|\beta_{(-2\pi\ell/a)}| > |\beta_{(-2\pi q/a)}|$ for all $q \neq \ell$. Therefore, as the shock front is broadened, $R(x) \rightarrow \beta_{(-2\pi/a)} e^{i(2\pi x/a)}$ for light reflecting from the first band gap. The reverse Doppler shift scenario in Fig. 3 corresponds to this case where the only dominant component of $R(x) = \sum_G \beta_G e^{-iGx}$ is the one corresponding to $G = -2\pi/a$. Other frequency components of $R(x)$ are suppressed by the relatively broad shock front width in this case. Equations (5) and (6) indicate that the reflected light should have a single frequency with a negative shift if $v > 0$, $k_0 > 0$, and $|2k_0| < 2\pi/a$, which is the case in Fig. 3. In Fig. 4, the relatively sharp shock front gives rise to multiple reflected frequencies separated by $\frac{2\pi v}{a}$.

Equation (5) predicts that, when $2k_0 = -G$ and there is only one reflected frequency component, the Doppler shift is zero. Likewise, if $2k_0 > -G$, the Doppler shift

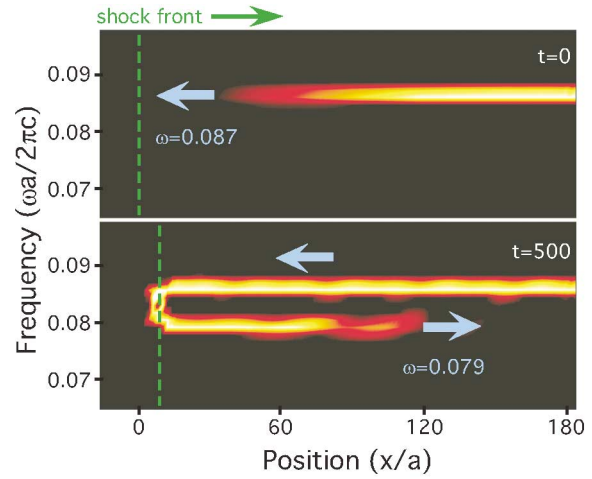


FIG. 3 (color). Reverse Doppler effect. Two moments in time during a computer simulation of a pulse of light reflecting from a time-dependent dielectric similar to Fig. 1. The shock front is moving to the right and its location is approximately indicated by the dotted green line. Light incident from the right receives a negative, i.e., *reversed*, Doppler shift upon reflection from the shock wave. Time is given in units of a/c .

is positive (normal) but has a magnitude that is smaller than the usual $2k_0 v$ Doppler shift. Both of these scenarios have been observed in our finite-difference simulations.

We would like to emphasize that it is not possible to observe these anomalous effects by simply translating a photonic crystal through a uniform medium because the reflection coefficient for the photonic crystal in that case is constant, as in the case of a metal mirror. The key new physical phenomena presented here result from the fact

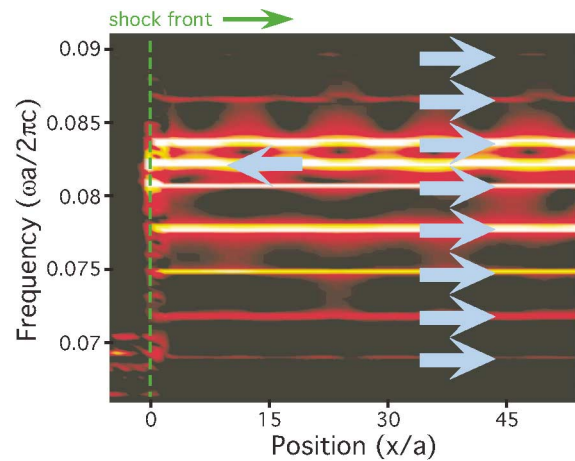


FIG. 4 (color). Computer simulation of a pulse of light reflecting from a dielectric similar to Fig. 1, but with a sharper shock front than in Fig. 3 (by a factor of 20). The shock front is moving to the right and its location is approximately indicated by the dotted green line. Light incident from the right is reflected in multiple equally spaced frequencies due to the relatively sharp shock front.

that the shocked photonic crystal region “grows” into the preshocked region giving rise to a time-dependent reflection coefficient. It is also interesting to note that the velocity of the material behind the shock front plays no role in the Doppler shift phenomenon. Only the shock front velocity is relevant.

In the finite-difference simulations, we have chosen a 10 GPa shock with large shock speeds and large strain dependence of the dielectric due to consideration for computational effort. The effects presented here are just as easily observable over a wide range of shock pressures, realistic shock speeds (1–10 km/sec), and realistic values of $\frac{1}{\epsilon} \frac{d\epsilon}{ds}$. Materials are routinely shocked to GPa and higher pressures using lasers and gun facilities. Optical techniques involving the reflection of light from a moving shock front are used as diagnostics in shock experiments [8,9]. Spectroscopic techniques possess ample resolution to observe the shifts proposed here which are comparable to a normal Doppler shift from an object moving on the order of 100 m/s [10]. It is also interesting to note that measurement of the properties of the reflected light in such an experiment allows determination of the shock front thickness as in Figs. 3 and 4. This is currently difficult or impossible to accomplish in present-day experiments and is a new tool for the study of shock waves.

For small shock pressures, the requirement that the light be in the linear dispersion frequency region of the preshocked crystal (away from the band edge) can be accomplished by using a crystal with a small band gap, e.g., by using a large layer of a material with large negative $\frac{d\epsilon}{ds}$ and a small layer of another material with a different dielectric. In this case, the condition on $\frac{d\epsilon}{ds}$ for the band gap to decrease upon compression is $\frac{1}{\epsilon} \frac{d\epsilon}{ds} < -2$. Materials used for acoustic light modulation, such as Te, or other high dielectric materials can be used to satisfy this condition. Alternatively, if light is reflected from the rear of the shock front (i.e., the incident light propagates the same direction as the shock), materials with $\frac{1}{\epsilon} \frac{d\epsilon}{ds} > -2$ (i.e., all other materials) can be employed to observe a reversed Doppler shift if the incident light is of a frequency within the band gap of the preshock crystal.

Shock impedance matching between the two bilayers of the photonic crystal is important for the propagation of a steady shock wave. A wide variety of optical materials of varying impedances exist to simultaneously establish good impedance matching and dielectric contrast, for example, Te and LiF. These two materials are not required to possess identical sound speeds because the reflection coefficient $R(x)$ is periodic in time even when the sound speeds differ. Differing elastic moduli between the two

materials has little effect on the gap position when one of the bilayers is substantially smaller than the other.

While the emphasis of this work has been on the observation of anomalous Doppler shifts in a shocked photonic crystal, similar shifts can be observed in a variety of time-dependent photonic crystal systems. The key requirement is the time-dependent reflection coefficient discussed earlier. Materials that undergo a change in the dielectric constant under an applied electric field or applied change in temperature can be modulated in a time-dependent shocklike fashion, and micro-electro-mechanical systems may also be used to observe the same phenomena.

Finally, this work presents a new and general physical mechanism to manipulate and modulate the carrier frequency of light while performing the difficult task of preserving optical coherence. Potential applications for this technology include quantum information processing, all-optical signal processing, and new diagnostic tools for shock wave experiments.

The authors thank Neil Holmes, Jerry Forbes, and David Hare for helpful discussions. Evan Reed acknowledges support from the Department of Defense NDSEG, and the Lawrence Livermore National Laboratory MRI/EMC. This work was supported in part by the Materials Research Science and Engineering Center program of the National Science Foundation under Grant No. DMR-9400334.

*Electronic address: evan@mit.edu

- [1] E. Yablonovich, Phys. Rev. Lett. **58**, 1059 (1987); S. John, Phys. Rev. Lett. **58**, 2486 (1987); J. D. Joannopoulos, R. D. Meade, and J. N. Winn, *Photonic Crystals* (Princeton University Press, Princeton, NJ, 1995).
- [2] E. J. Reed, M. Soljacic, and J. D. Joannopoulos, Phys. Rev. Lett. **90**, 235503 (2003).
- [3] M. Einat and E. Jerby, Phys. Rev. E **56**, 5996 (1997).
- [4] V. G. Veselago, Sov. Phys. Usp. **10**, 509 (1968).
- [5] A. M. Belyantsev and A. B. Kozyrev, Tech. Phys. **47**, 1477 (2002).
- [6] A. Taflove and S. C. Hagness, *Computational Electrodynamics: The Finite-Difference Time-Domain Method* (Artech House, Norwood, MA, 2000).
- [7] R. W. Dixon, J. Appl. Phys. **38**, 5149 (1967).
- [8] R. Gustavsen and Y. M. Gupta, J. Appl. Phys. **69**, 918 (1991).
- [9] P. M. Celliers, G. W. Collins, L. B. D. Silva, D. M. Gold, R. Cauble, R. J. Wallace, M. E. Foord, and B. A. Hammel, Phys. Rev. Lett. **84**, 5564 (2000).
- [10] N. C. Holmes, Rev. Sci. Instrum. **64**, 357 (1993).